Measurements of the concentration and composition of nuclei for cirrus formation

P. J. DeMott*†, D. J. Cziczo‡§, A. J. Prenni*, D. M. Murphy‡, S. M. Kreidenweis*, D. S. Thomson‡§, R. Borys¶, and D. C. Rogers‖

*Department of Atmospheric Science, Colorado State University, Fort Collins, CO 80523; ‡Aeronomy Laboratory, National Oceanic and Atmospheric Administration, Boulder, CO 80305; §Cooperative Institute for Research in Environmental Sciences, University of Colorado, Boulder, CO 80309; ¶Storm Peak Laboratory, Desert Research Institute, P.O. Box 770799, Steamboat Springs, CO 80477; and ‖National Center for Atmospheric Research, Boulder, CO 80307

Edited by A. R. Ravishankara, National Oceanic and Atmospheric Administration, Boulder, CO, and approved October 14, 2003 (received for review May 5, 2003)

This article addresses the need for new data on indirect effects of natural and anthropogenic aerosol particles on atmospheric ice clouds. Simultaneous measurements of the concentration and composition of tropospheric aerosol particles capable of initiating ice in cold (cirrus) clouds are reported. Measurements support that cirrus formation occurs both by heterogeneous nucleation by insoluble particles and homogeneous (spontaneous) freezing of particles containing solutions. Heterogeneous ice nuclei concentrations in the cirrus regime depend on temperature, relative humidity, and the concentrations and physical and chemical properties of aerosol particles. The cirrus-active concentrations of heterogeneous nuclei measured in November over the western U.S. were <0.03 cm^{-3}. Considering previous modeling studies, this result suggests a predominant potential impact of these nuclei on cirrus formed by slow, large-scale lifting or small cooling rates, including subvisual cirrus. The most common heterogeneous ice nuclei were identified as relatively pure mineral dusts and metallic particles, some of which may have origin through anthropogenic processes. Homogeneous freezing of large numbers of particles was detected above a critical relative humidity along with a simultaneous transition in nuclei composition toward that of the sulfate-dominated total aerosol population. The temperature and humidity conditions of the homogeneous nucleation transition were reasonably consistent with expectations based on previous theoretical and laboratory studies but were highly variable. The strong presence of certain organic pollutants was particularly noted to be associated with impedance of homogeneous freezing.

The indirect effects of aerosol particles on the radiation budget of the earth are highly uncertain both in magnitude and in the direction of the forcing (1). The formation and persistence of high-altitude tropospheric ice clouds (cirrus) have been shown to be particularly important factors in global climate control (2). Studies of central importance in this regard are investigations of how aerosols modulate the cloud ice phase and determination of the significance of anthropogenic aerosol contributions and their variability on ice nucleation (1).

Indirect effects of aerosol particles on cirrus clouds derive from ice-formation processes and alteration of cloud microphysical properties. Cirrus cloud radiative properties are very sensitive to the size, concentration, phase, and shape of the cloud particles (3). Understanding the effects of aerosol particles on cirrus is complicated by the fact that multiple ice-formation mechanisms are possible, and vapor-phase mass transfer can limit both nucleation and ice-crystal growth (4). Thus, for example, the presence of more effective ice nuclei (IN), in some cases, may lead to a decrease in ice-crystal number density (5–7), but the impact on radiative transfer could be modulated by an increase in crystal size and subsequent increase in sedimentation rates. It therefore is important to identify the key ice-nucleation processes, their source particle populations, and potential impacts on these processes.

At cirrus temperatures (−30 to −80°C), nucleation of ice particles can occur by the homogeneous-freezing nucleation of liquid particles and by the heterogeneous catalytic action of insoluble IN (8). Homogeneous freezing involves spontaneous ice-embryo formation within soluble aerosol particles in various states of dilution (9). When the formation of cirrus is driven by deep convection, cloud droplets can remain liquid until they homogeneously freeze at the expected condition for pure water below −36°C (10). For cirrus forming in place in the upper troposphere, homogeneous freezing is expected to occur in increasingly concentrated solution drops as temperature decreases below −36°C (11, 12). The freezing condition as a function of particle composition leads to a fairly well defined regime of water subsaturated and ice supersaturated conditions in which cirrus is predicted to form homogeneously. Heterogeneous ice nucleation in particles that are wholly insoluble or partially soluble can potentially cause cirrus formation at warmer temperatures and lower relative humidity (5). Hypothesized heterogeneous ice-nucleation mechanisms include deposition nucleation (ice embryos form from the vapor on a surface), condensation freezing (ice formation during liquid condensation), immersion freezing (freezing by a particle previously immersed in a liquid drop), and contact freezing (freezing initiated by an aerosol particle collision with a liquid drop). Certain physical and chemical properties seem requisite for insoluble particles to act as IN (13).

Past studies of IN compositions have collected ice crystals on the ground or from clouds and analyzed the core nuclei by using electron microscopy. Analyses of the central nuclei of snow crystals have identified clay particles (14) and Asian mineral dusts (15) as important atmospheric IN. Microscopy measurements of the elemental compositions of evaporated residual nuclei from cirrus ice crystals indicated the enrichment of metals and other heavy elements and depletion of lighter elements such as sulfur in crystal residual particles compared to out-of-cloud particles (16). Similar analyses of the residual nuclei from ice crystals formed on aerosol particles in an ice nucleus-processing instrument (earlier version of the one used in the current study) indicated the strong enrichment of silicates in IN compared to the predominant sulfates in the ambient upper tropospheric aerosol population (17). Processing temperature was limited to warmer than −37°C in that study, so much of the cirrus cloud regime was not sampled, and homogeneous-freezing nucleation was not examined. Recent airborne IN measurements (18), also at temperatures warmer than −35°C, indicate elevated IN concentrations within Saharan dust layers. Lidar studies have documented the strong cloud-glaciating effect of dust particles from both Asian and Saharan sources (19, 20). Laboratory

This paper was submitted directly (Track II) to the PNAS office.

Abbreviations: IN, ice nuclei; PALMS, particle analysis by laser MS; CFDC, continuous-flow diffusion chamber; GMT, Greenwich mean time; RH_i, ice relative humidity; RH_w, water relative humidity.

†To whom correspondence should be addressed. E-mail: pdemott@lamar.colostate.edu.

studies using surrogates for airborne crustal and mineral dust particles predict the strong ice-nucleation efficiency of such particles throughout the cirrus cloud temperature regime (21–23).

Results are presented in this study from a system that processes aerosol particles to induce ice nucleation under well defined conditions across the cirrus cloud regime and analyzes the residual nuclei of the freshly nucleated ice crystals by using a single-particle mass spectrometer (24). Both insoluble and volatile species are detected, which is not the case using electron microscopy, and detection occurs in real time. The homogeneous and heterogeneous ice-nucleation activity of particles is assessed in real time and is correlated to their aerosol chemical composition.

Methods

General Procedures. Aerosol sampling was conducted at Storm Peak Laboratory, located on Mt. Werner (elevation 3,200 m above mean sea level) in western Colorado (25). The key motivation for using this site was its ready access and direct exposure to free tropospheric air for extended periods of time. The experimental sampling period occurred from November 1 to 19, 2001.

The general experimental methodology applied for this study has been described by Cziczo *et al*. (24). Aerosol particles were either sampled directly by the particle analysis by laser mass spectrometry (PALMS) single-particle analyzer to determine overall particle ionic compositions or were first passed to a continuous-flow diffusion chamber (CFDC) to induce ice nucleation in aerosol particles at defined temperature and humidity conditions. An inline counterflow virtual impactor was used to isolate nucleated ice crystals leaving the CFDC and permit PALMS analysis of the ionic mass spectral composition of crystal residual nuclei. Ambient aerosols were drawn from ≈10 m above ground level through a cyclone impactor with a nominal 0.75-μm cut size, as validated by an optical particle counter. The removal of larger aerosols is necessary for CFDC measurements (26). Sample air was dehydrated by passing it through a 50-cm length of Nafion (DuPont) tubing (Perma Pure, Toms River, NJ) that used dry N_2 gas to extract water vapor from the sample air.

CFDC Processing of Aerosol Particles. The CFDC instrument is described by Rogers *et al*. (26) and references therein. It was modified for this study to operate to temperatures below −60°C and to use N_2 as sheath air (24). The instrument focuses an aerosol particle stream into the central portion (≈10% of volume) of vertically downward-oriented laminar flow between two ice-coated cylindrical walls held at different temperatures. The interwall temperature gradient and vapor field allow for aerosol stream exposure to constant temperature (±0.7°C precision, 1°C maximum difference across aerosol lamina) and relative humidity (±0.6% precision with respect to water, 2% maximum difference across aerosol lamina) conditions for a period (5–7 s in this study) that permits ice nucleation and growth to occur. A hydrophobic material replaces ice on the warmer wall in the lower third of the CFDC to evaporate liquid particles, including cloud droplets. Detection of ice formation is by optical measurement of preferentially grown ice particles as they leave the CFDC. Deposition, condensation-freezing, immersion-freezing, and homogeneous-freezing nucleation processes can occur in this instrument.

Aerosols were processed in the CFDC across a range of temperature and humidity values representative of cirrus. The inline counterflow virtual impactor (24) extracted those ice crystals nucleated and grown to sizes >1.5 μm. The crystals evaporated at room temperature (typically 15°C) during transit to the PALMS instrument. The inline counterflow virtual impactor was sometimes replaced by an inertial impactor (24) with a 1.5-μm cut size that permitted sampling of ice crystals onto transmission electron microscopy grids for analysis of residual particles.

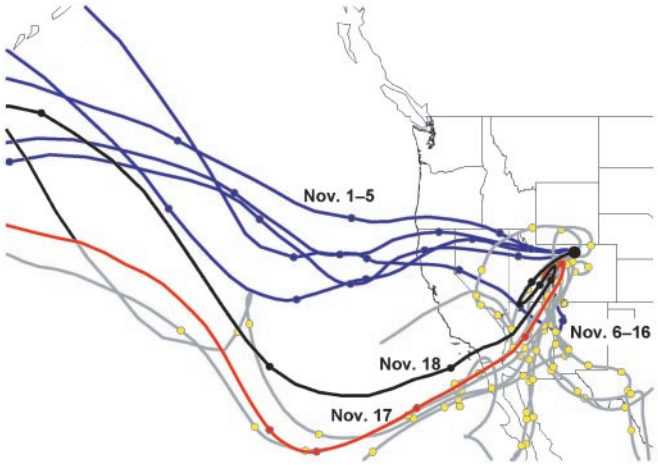

Fig. 1. Seven-day back-trajectory analyses from the measurement site initialized at 12:00 GMT (except 00:00 GMT on November 18). Color-coded time periods are discussed in *Results and Discussion*. Filled circles mark daily units of each trajectory.

PALMS Measurements. The PALMS instrument has been described by Thomson *et al*. (27). Aerosol particles are drawn by vacuum into PALMS. A fraction of these particles are detected by a visible light laser (λ = 532 nm), the scattered light from which triggers an excimer laser (λ = 193 nm) that ablates and ionizes individual particles. A complete positive or negative mass spectrum is obtained on particles by using a time-of-flight mass spectrometer.

Ancillary Measurements. Additional aerosol particle measurements were obtained for detecting times of suspected impact of pollution and for correlating to the IN measurements. Measurements included total particle concentrations at sizes above ≈5 nm (TSI model 3025, St. Paul), scanning mobility particle sizer (TSI, St. Paul) measurements of aerosol size distributions between 10 and 300 nm, and size distributions between 0.5 and 20 μm obtained by aerodynamic sizing (TSI model 3321). Fine-particle mass and bulk elemental and ionic composition data for 24-h periods at 3-day intervals were available from a nearby Interagency Monitoring Program for Visual Environments (http://vista.cira.colostate.edu/improve) network sampling site. This site, in the Mt. Zirkel Wilderness (longitude: 106.6765 W; latitude: 40.5383 N; elevation: 3,243 m), is just north of and at a similar elevation as the Storm Peak Laboratory (longitude: 106.73W; latitude: 40.45 N; elevation: 3,220 m).

Results and Discussion

Air Mass and Ambient Aerosol Characterization. The sampling period was characterized for air mass and aerosol characteristics to place the IN measurements in context. Seven-day back-trajectory calculations for the sampling period were done by using the National Oceanic and Atmospheric Administration Climate Modeling and Diagnostics Laboratory isentropic trajectory model (28). Fig. 1 shows a summary of trajectories initialized daily at 12:00 Greenwich mean time (GMT). These indicate that the sampling site was receiving air in a strong, westerly flow (blue lines) for relatively few days during the project period. It was more typically the case that air resided over the western and southwestern United States for 4–5 days preceding aerosol sampling (gray lines with yellow points), reflect-

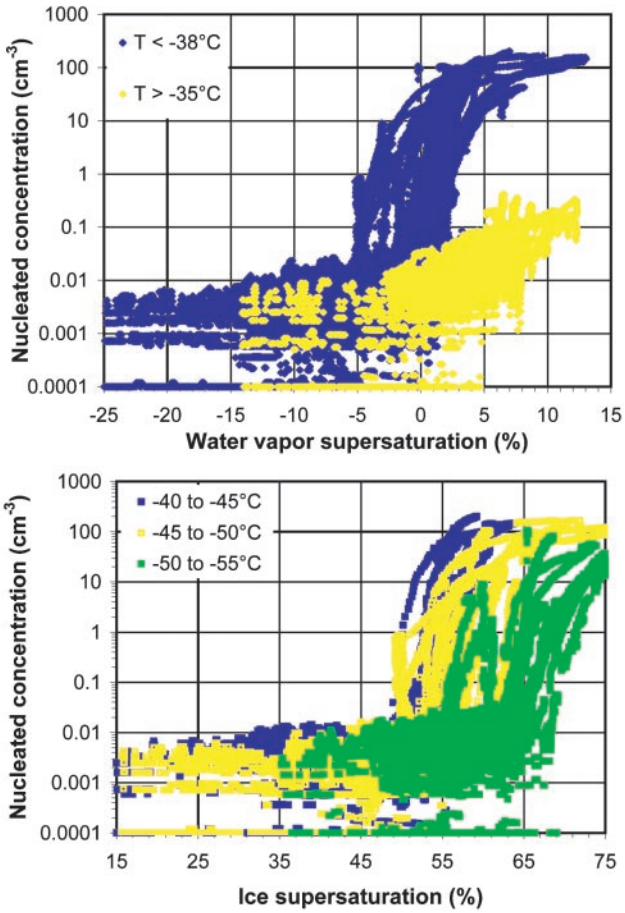

Fig. 2. Ice concentrations nucleated by or within aerosol particles as a function of water vapor supersaturation (*Upper*) and ice supersaturation (*Lower*) for the project period. Data are color-coded to differentiate measurements in different temperature regimes. Increases in nucleated concentrations at near water saturation and at higher ice supersaturation conditions are indicative of homogeneous freezing at temperatures below −38°C.

ing high pressure and large-scale subsidence over the western United States. Only two precipitation events occurred during the period.

Dust transports are of particular interest because of previous indications of the importance of crustal elements as potential IN. Average soil dust concentrations during the project period were 0.25 ± 0.16 $\mu g \cdot m^{-3}$ based on Interagency Monitoring Program for Visual Environments data. These compare to 3-year average soil dust concentrations of 0.59 ± 0.16 $\mu g \cdot m^{-3}$ and the peak soil dust concentrations from 1 to as high as 20 $\mu g \cdot m^{-3}$ that occur during spring to summer because of Asian dust influences at this site and in the Rocky Mountain region in general (29).

Homogeneous and Heterogeneous Ice Nucleation. The concentrations of ice nucleating on aerosol particles during the project period are plotted as a function of water and ice supersaturation (relative humidity with respect to water or ice minus 100%) in Fig. 2. These data represent 36.4 h of 1-Hz data processed as 30-s running mean concentrations. Data are color-coded in Fig. 2 by temperature regimes. Fig. 2 *Upper* distinguishes data warmer than −35°C versus colder than −38°C. The reason for this segregation is the fact that −38°C is roughly the threshold temperature for detecting homogeneous freezing of activated cloud droplets for the residence time in the CFDC, and this process is not statistically probable at temperatures above approximately −35°C (13).

Nearly discontinuous increases in ice formation versus water supersaturation, near but typically <0% (water saturation), is noted when ambient aerosol particles were processed colder than −38°C (Fig. 2 *Upper*). This reflects a fundamental change from ice formation on a limited population of heterogeneous IN to homogeneous ice formation. Nucleated concentrations ultimately exceed 100 cm^{-3}, representing ≈1 in 10 of all aerosol particles nucleating ice in the CFDC residence time. Note that higher supersaturations were sometimes required to achieve the highest nucleation rates because smaller and/or less hygroscopic particles require this condition for dilution to the degree necessary for freezing. An instrumental factor in this regard may be the limited residence time provided for condensational and ice-growth kinetics of the smallest or most hydrophobic particles. This factor is not critical to detecting the onset of homogeneous freezing.

The Fig. 2 *Lower* shows a portion of the lower temperature data (less than −40°C) segregated into 5°C temperature bins and plotted versus ice supersaturation. This data representation shows that homogeneous freezing requires a somewhat higher ice supersaturation as temperature decreases. The onset of homogeneous freezing versus relative humidity in this manner is expected from theoretical and numerical studies (ref. 4 and references therein), has been demonstrated by laboratory studies by using model sulfate aerosol particles (11, 30), and has been inferred indirectly from cloud measurements (31–34). These are direct measurements of the critical conditions for homogeneous freezing by ambient aerosol particles. A 100-nm pure sulfate particle is expected to freeze homogeneously at 150.5%, 154.2%, and 158.5% ice relative humidity (RH_i) at processing temperatures of −42.5, −47.5, and −52.5°C, respectively, based on laboratory studies (11, 12). Larger particles have a lower onset relative humidity and vice versa. The average onset conditions for homogeneous freezing indicated on natural aerosols in Fig. 2 are 152%, 155%, and 162% RH_i at the noted temperatures. These values are generally higher than but still in good agreement with predictions. The RH_i values are also in line with the maximum RH_i values observed in the upper troposphere in some studies (35). Nevertheless, a wide spread of activation conditions is noted within each temperature range. The spread is greater than can be explained by differences in temperature alone.

Heterogeneous IN concentrations of <0.01 cm^{-3} (median value) are indicated in Fig. 2 at processing temperatures below −38°C. Only weak dependencies on water relative humidity (RH_w) or RH_i (directly) and temperature (inversely) were observed in this regime. These dependencies will be quantified in a separate article. Previous numerical model studies have indicated that, in addition to vertical velocity, the numbers of available IN at lower ice supersaturations are critical to determining the dominant ice-formation process in cirrus forming in place (5–7, 31, 36). The presence of IN can lower the concentrations of ice nucleated in cirrus by vapor-phase depletion such that peak relative humidity is reduced and homogeneous freezing does not occur. For the IN concentrations noted at the time and location of this study, this competitive scenario seems possible for cirrus generated in updrafts of less than ≈10 $cm \cdot s^{-1}$ or for equivalent cooling rates (5–7, 31, 36). This includes cirrus forming in synoptic-scale vertical-motion fields and the subvisual or thin cirrus found over wide areas of the globe at high altitudes (35). IN concentrations exceeding 0.1 cm^{-3}, in contrast, would be required to affect cirrus forming in updrafts on the order of 50 $cm \cdot s^{-1}$ (36), which encompasses much of the range-of-wave motions that may be responsible for cellular generation of widespread cirrus (37).

Ice concentrations increase to >0.1 cm^{-3} at $RH_w > 100\%$ up to ≈105% in the warmer cirrus regime (warmer than −35°C), under which only heterogeneous ice nucleation can occur. This result reflects an increase in the numbers of heterogeneous IN

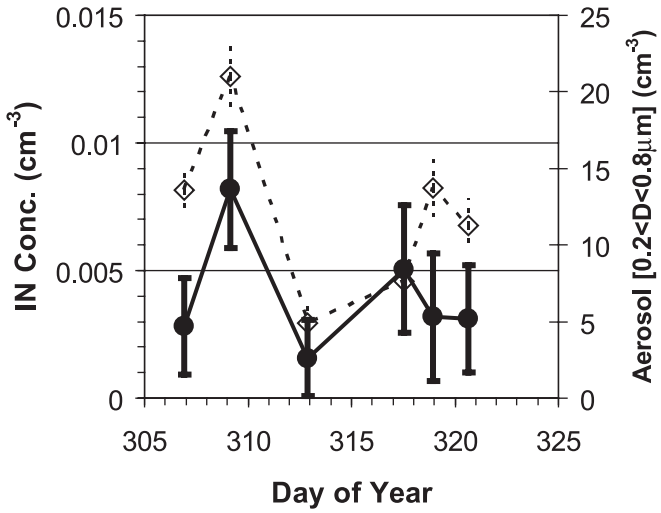

Fig. 3. Heterogeneous IN concentrations (filled symbols) for selected conditions (−42 to −46°C and 90–92% RH_W) and ambient aerosol concentrations (open symbols) in a selected size range (200–800 nm) as a function of time.

activating by condensation or immersion freezing as supersaturation increases. The fact that all particles, including relatively hydrophobic ones, will condense dilute water drops above some RH_w (≈105% here) leads to an apparent upper limit for nucleated concentrations by heterogeneous freezing. This observation is consistent with a previous CFDC study at these temperatures (31). These results have relevance to heterogeneous nucleation contributions to ice in cold anvil clouds forming at the top of deep convective clouds but will not be discussed further here.

The generality of inferences obtained regarding heterogeneous IN concentrations and cirrus clouds depends on how IN concentrations change due to changes in their (unknown) source contributions over time and seasons. It was observed that IN concentrations vary with changes in the size distribution of the total aerosol (Fig. 3). The data in Fig. 3 have been selected for the specific temperature and relative humidity ranges noted in the caption, but the result was valid for any narrowly defined subset of data. For such selections, higher aerosol concentrations within the size range that includes IN (typically >100 nm based on transmission electron microscopy samples) lead in general to increases in IN concentrations and vice versa, although the relationship is not simply linear. Coagulation, cloud processing, and precipitation scavenging of particles must also play a role.

Ice-Crystal Residual Particle Compositions. Observed total aerosol and residual nuclei compositions were broadly grouped into six major statistical categories as shown in Fig. 4. Categories were produced by using cluster analysis to combine positive and negative ion mass spectra with similar components (38), with names based on the predominant features. The background or total aerosol particle population was dominated by particles with a sulfate and organic composition (86%) with lesser contributions from particles with potassium and carbon (frequently associated with biomass burning, 9%), carbon and vanadium (often associated with combustion sources, 2.2%), mineral dust or fly ash (1.0%), metallic particles (1.6%), and other types (0.2%). Particles that nucleated ice under conditions conducive to both homogeneous and heterogeneous ice nucleation exhibit a similar percentage composition to the total particle population, whereas particles that nucleated ice under conditions favorable to only heterogeneous nucleation had the most varied compositional makeup and a lower percentage of particles dominated by sulfate. In this latter case, the sulfate was often the predominant peak among less resolved peaks for insoluble species or may have been the coating of an insoluble particle that is more readily ionized by the PALMS technique. Large contributions from mineral dust or fly ash (33%) and metallic (25%) particles are noted in the heterogeneously nucleated particles, suggesting strong natural and anthropogenic inputs to IN populations. Analysis of ice-crystal residuals by transmission electron microscopy provided additional information for source speciation. Using a high degree of particle sphericity as a criterion for identifying fly ash particles, transmission electron microscopy results indicated that 20% of the mineral dust/fly ash category had a likely source from industrial processes, whereas 80% were likely of natural mineral dust origin. The mineral dust/fly ash particles were relatively pure in form, with only ≈25% containing measurable sulfate and organics.

Unusual Apparent Chemical Effects on Homogeneous-Freezing Nucleation. We investigate here the possibility that aerosol particle chemistry factors into causing the wide variation in the onset conditions of homogeneous freezing noted at similar temperatures in Fig. 2. Data plotted for individual days in Fig. 5 contrast with the onset conditions for homogeneous freezing between a more typical day (November 3) and the project day that showed the most unusual chemical compositions (November 17). The water supersaturation conditions for homogeneous freezing as predicted by laboratory studies (10, 11) for pure 100-nm ammonium sulfate particles at the processing temperatures are shaded into each panel of Fig. 5. The observed onset of homogeneous freezing on November 3 is consistent with expec-

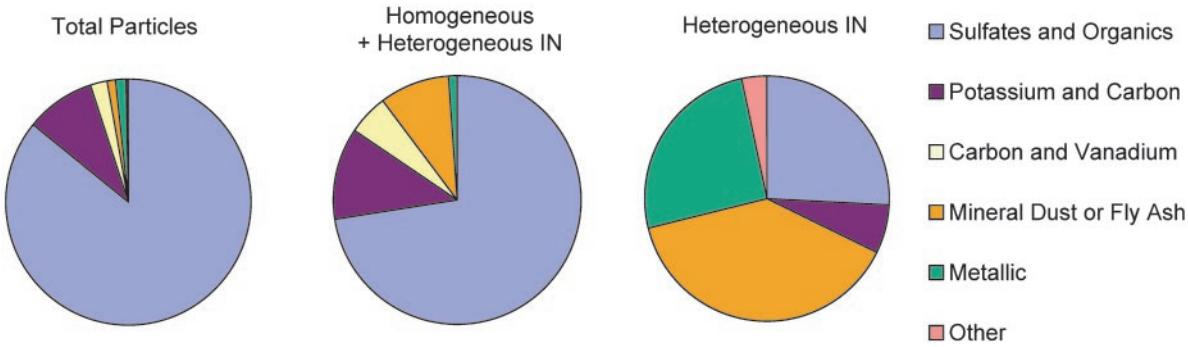

Fig. 4. Statistics of different particle populations based on cluster analysis of PALMS mass spectra. The total aerosol composition is shown (*Left*), and the composition of nucleated ice-crystal residuals are shown in the regime under which homogeneous freezing was dominating heterogeneous nucleation (*Center*) and under conditions favorable only to heterogeneous nucleation (*Right*).

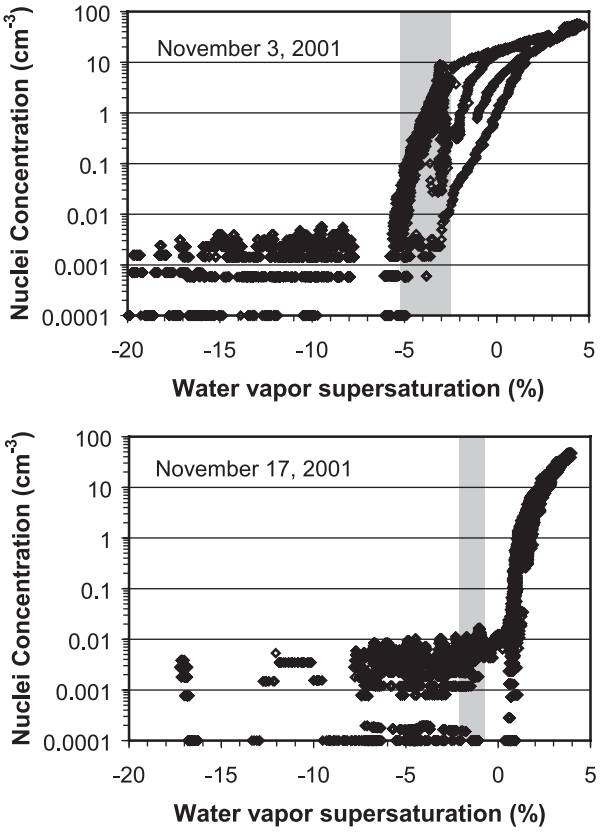

Fig. 5. Comparison of the conditions required for homogeneous freezing of ambient aerosols on November 3 (−51°C nominal processing temperature) and November 17 (−44°C nominal processing temperature). The shaded regions indicate the expected conditions for homogeneous freezing (onset to complete freezing) of pure sulfate aerosols for the range of CFDC processing temperatures on each day.

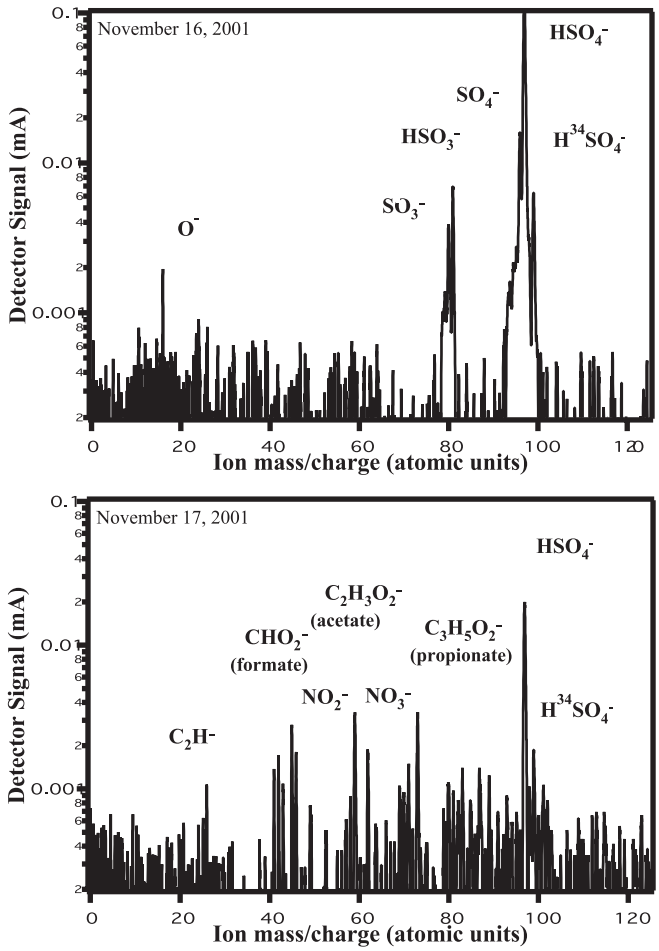

Fig. 6. PALMS negative ion mass spectra of ice-crystal residual particles typical of homogeneous-freezing conditions in two different types of air masses. (*Upper*) A negative polarity spectrum obtained on November 16. This particle, as well as the background aerosol, had minimal organics, instead being relatively pristine sulfates. Conversely, *Lower* shows a negative polarity spectrum obtained on November 17 that also coexhibits several organic fragments (as did the background aerosol) with sulfate.

tations for sulfate particles. The onset of freezing on November 17 occurs at a much higher relative humidity than expected.

The different results shown in Fig. 5 may reflect the different overall particle composition observed for these two days. The background aerosol particles on November 17 contained the most organic, nitrate, and ammonium components of any sample day. Fig. 6 compares a representative negative polarity mass spectrum from a homogeneously nucleated ice-crystal residual particle on November 17 with one that was more reflective of project average compositions. The typical negative polarity spectrum had minimal organic signature, instead being relatively pristine sulfates. Conversely, the negative polarity spectrum obtained on November 17 coexhibits several organic fragments with sulfate. Positive polarity spectra of homogeneously nucleated particles on November 17 also exhibited several organic fragments not frequently observed on other days.

Sampling on November 17 was conducted in the evening during a transition from long-range air mass sources west of Baja, CA to a region further north (compare 00:00 GMT trajectory on November 18, or early evening local time on November 17, and 12:00 GMT trajectory on November 17). During the transition, vertical positions of trajectories (data not shown) indicate the possible transport of lower-level air from southern California metropolitan regions or other populated regions to the site. This suggests at least an opportunity for bringing pollutants to the site.

The association of the presence of organic species in particles with impeding effects on homogeneous freezing is loosely consistent with the only available laboratory studies of organic effects on homogeneous freezing. Laboratory studies by Prenni *et al*. (39) indicate that some pure and soluble dicarboxylic acids homogeneously freeze at higher relative humidity than equivalent-sized sulfate particles at a given temperature. It is not clear at the present time whether organic species present as solutes, surface films, or insoluble components might affect ice-embryo formation in a fundamental manner or affect the kinetics of water uptake required for ice formation.

Conclusions and Implications

The use of a unique coupled system for simultaneously detecting the concentration and composition of aerosols initiating ice formation has provided information relevant to the indirect effect of aerosols on cirrus clouds.

- The concentrations of particles active as heterogeneous IN under cirrus formation conditions depended directly on supersaturation (with respect to water or ice) and aerosol concentrations at sizes above ≈0.1 μm and indirectly on temperature. Quantitative analyses are forthcoming.
- Typical IN concentrations were <0.01 cm^{-3} in free tropospheric air during the sampling period. These IN concentrations are similar to those assumed in previous modeling calculations that indicated heterogeneous nucleation effects

GEOPHYSICS

on a subset of cirrus clouds: those forced by slow ascent (<10 cm·s^{-1}) or those forming in dynamical situations leading to low or limited cooling rates (e.g., subvisual or thin cirrus). Estimation of the global impact of the measured heterogeneous IN concentrations will require further quantification of results, incorporation into appropriate numerical models, and high-resolution information on the global distribution of vertical motion and water vapor fields in the upper troposphere.

- Heterogeneous IN populations are dominated by insoluble components of atmospheric particles, as expected. Primary contributors to their concentrations are particles with mineral dust/fly ash origins and metallic particles, suggesting strong natural and anthropogenic (industrial or combustion) inputs. IN concentrations are expected to be enhanced when atmospheric mineral particle concentrations increase because of natural or anthropogenic factors. The sampling period in this study was characterized by quite-low, fine dust mass.
- Background aerosol particles were observed to freeze homogeneously as haze particles in large numbers at low temperatures (less than −38°C) and at humidity conditions generally expected for sulfates based on prior laboratory studies. Nevertheless, the onset temperature and relative humidity conditions for homogeneous freezing were quite variable.
- The presence of organic ionic fragments in nucleated particles was associated with a requirement of much higher relative humidity for homogeneous ice formation in internally mixed organic-sulfate aerosol particles. The reason for this effect is not known yet.

These conclusions indicate a number of issues that deserve further investigation. More data are needed to determine seasonal and temporal patterns and thereby lead to recommendations for robust parameterizations of ice-nucleation processes in cloud, regional, and global-scale models. Particular issues requiring further study in the laboratory and the atmosphere include the role of different desert dust sources and dust loadings on heterogeneous ice nucleation and elucidation of how freezing nucleation is impeded in internally mixed organic/sulfate aerosols.

We are grateful to the National Parks Service for data from the Interagency Monitoring Program for Visual Environments network. We thank Katie Walters, Brian Jesse, Chuck Brock, J. Schreiner, Paula Hudson, Sarah Brooks, Melanie Wetzel, and the Steamboat Ski Area for assistance during the conduct of this research. We acknowledge Scot Martin and an anonymous reviewer for helpful critical comments. We gratefully acknowledge Joyce Harris of the National Oceanic and Atmospheric Administration Climate Modeling and Diagnostics Laboratory (CMDL) for providing isentropic trajectory data. The Desert Research Institute is an equal opportunity provider and employer and is a permittee of the Medicine-Bow and Routt National Forest. This work was supported by National Science Foundation Grants ATM0124927 and ATM0071321 and National Oceanic and Atmospheric Administration base funding.

1. Intergovernmental Panel on Climate Change (2001) in *Climate Change 2001: The Scientific Basis*, eds., Houghton, J. T., Ding, Y., Griggs, D. J., Noguer, M., van der Linden, P. J., Dai, X., Maskell, K. & Johnson, C. A. (Cambridge Univ. Press, Cambridge, U.K.), pp. 291–335.
2. Liou, K.-N. (1986) *Mon. Weather Rev.* **114,** 1167–1199.
3. Stephens, G. L., Tsay, S., Stackhouse, P. W., Jr., & Flatau, P. J. (1990) *J. Atmos. Sci.* **47,** 1742–1753.
4. Lin, R.-F., Starr, D. O. C., DeMott, P. J., Cotton, R., Sassen, K., Jensen, E., Kärcher, B. & Liu, X. (2002) *J. Atmos. Sci.* **59,** 2305–2329.
5. DeMott, P. J., Rogers, D. C. & Kreidenweis, S. M. (1997) *J. Geophys. Res.* **102,** 19575–19584.
6. Jensen E. J. & Toon, O. B. (1997) *Geophys. Res. Lett.* **24,** 249–252.
7. Kärcher, B. & Lohmann, U. (2003) *J. Geophys. Res.* **108,** 4402, 10.1029/2002JD003220.
8. DeMott, P. J. (2002) in *Cirrus*, eds. Lynch D. K., Starr, D. O. C., Sassen, K. & Stephens, G. (Oxford, New York), pp. 102–135.
9. Martin, S. T. (2000) *Chem. Rev. (Washington, D.C.)* **100,** 3403–3453.
10. Rosenfeld, D., Rudich, Y. & Lahav, R. (2001) *Proc. Natl. Acad. Sci. USA* **98,** 5975–5980.
11. Chen, Y., DeMott, P. J., Kreidenweis, S. M., Rogers, D. C. & Sherman, D. E. (2000) *J. Atmos. Sci.* **57,** 3752–3766.
12. Koop, T., Luo, B. P., Tsias, A. & Peter, T. (2000) *Nature* **406,** 611–614.
13. Pruppacher, H. R. & Klett, J. D. (1997) *Microphysics of Clouds and Precipitation* (Kluwer, Norwell, MA), 2nd Ed.
14. Kumai, M. (1961) *J. Meteorol.* **18,** 139–150.
15. Isono, K., Komabayasi, M. & Ono, A. (1959) *J. Meteorol. Soc. Jpn.* **37,** 211–233.
16. Heintzenberg, J., Okada, K. & Strom, J. (1996) *Atmos. Res.* **41,** 81–88.
17. Chen, Y., Kreidenweis, S. M., McInnes, L., Rogers, D. C. & DeMott, P. J. (1998) *Geophys. Res. Lett.* **25,** 1391–1394.
18. DeMott, P. J., Sassen, K., Poellot, M., Baumgardner, D., Rogers, D. C., Brooks, S. D., Prenni A. J. & Kreidenweis, S. M. (2003) *Geophys. Res. Lett.* **30,** 1732, 10.1029/2003GL017410.
19. Sassen, K. (2002) *Geophys. Res. Lett.* **29,** 1465, 10.1029/2001GL014051.
20. Sassen, K., DeMott, P. J., Prospero, J. M. & Poellot, M. R. (2003) *Geophys. Res. Lett.* **30,** 1633, 10.1029/2003GL017371.
21. Zuberi, B., Bertram, A. K., Cassa, C. A., Molina, L. T. & Molina, M. J. (2002) *Geophys. Res. Lett.* **29,** 1504, 10.1029/2001GL014289.
22. Hung, H. M., Malinowski, A. & Martin, S. T. (2003) *J. Phys. Chem. A* **107,** 1296–1306.
23. Archuleta, C. A. (2003) MS thesis (Dept. of Atmospheric Science, Colorado State University, Fort Collins).
24. Cziczo, D. J., DeMott, P. J., Prenni, A. J., Jesse, B., Kreidenweis, S., Hudson, P. K., Schreiner, J., Thomson, D. S., Brock, C. S. & Murphy, D. M. (2003) *Aerosol Sci. Technol.* **37,** 460–470.
25. Borys, R. D. & Wetzel, M. A. (1997) *Bull. Am. Meteorol. Soc.* **78,** 2115–2123.
26. Rogers, D. C., DeMott, P. J., Kreidenweis, S. M. & Chen, Y. (2001) *J. Atmos. Oceanic Technol.* **18,** 725–741.
27. Thomson, D. S., Schein, M. E. & Murphy, D. M. (2000) *Aerosol Sci. Technol.* **33,** 153–169.
28. Harris, J. M. & Kahl, J. D. W. (1994) *J. Geophys. Res.* **99,** 25845–25855.
29. Vancuren, R. A. & Cahill, T. A. (2002) *J. Geophys. Res.* **107,** 4804, 10.1029/2002JD002204.
30. Möhler, O., Stetzer, S., Schaefers, S., Linke, C., Schnaiter, M., Tiede, M., Saathoff, H., Krämer, M., Mangold, A., Budz, T., *et al.* (2003) *Atmos. Chem. Phys.* **3,** 211–223.
31. DeMott, P. J., Rogers, D. C., Kreidenweis, S. M., Chen, Y., Twohy, C. H., Baumgardner, D., Heymsfield, A. J. & Chan, K. R. (1998) *Geophys. Res. Lett.* **25,** 1387–1390.
32. Heymsfield, A. J. & Miloshevich, L. M. (1995) *J. Atmos. Sci.* **52,** 4302–4326.
33. Ström, J, Strauss, B., Anderson, T., Schroeder, F., Heintzenberg, J. & Wendling, P. (1997) *J. Atmos. Sci.* **54,** 2542–2553.
34. Jensen, E. J., Toon, O. B., Tabazadeh, A. Sachse, G. W., Anderson, B. E., Chan, K. R., Twohy, C. H., Gandrud, B., Aulenbach, S. M., Heymsfield, A. J., *et al.* (1998) *Geophys. Res. Lett.* **25,** 1363–1367.
35. Jensen, E. J., Toon, O. B., Vay, S. A., Ovarlez, J., May, R., Bui, P. T., Twohy, C. H., Gandrud, B. W., Pueschel, R. & Schumann, U. (2001) *J. Geophys. Res.* **106,** 17253–17266.
36. Gierens, K. (2003) *Atmos. Chem. Phys.* **3,** 437–446.
37. Kärcher, B. & Ström, J. (2003) *Atmos. Chem. Phys.* **3,** 823–838.
38. Murphy, D. M., Middlebrook, A. M. & Warshawsky, M. (2003) *Aerosol Sci. Technol.* **37,** 382–391.
39. Prenni, A. J., DeMott, P. J., Kreidenweis, S. M., Sherman, D. E., Russell, L. M. & Ming, Y. (2001) *J. Phys. Chem. A.* **105,** 11240–11248.